Anomalous diffusion on random fractal composites

2007 J. Phys. A: Math. Theor. 40 11453

(http://iopscience.iop.org/1751-8121/40/38/002)

IOP PUBLISHING JOURNAL OF PHYSICS A: MATHEMATICAL AND THEORETICAL

J. Phys. A: Math. Theor. **40** (2007) 11453–11465 doi:10.1088/1751-8113/40/38/002

Anomalous diffusion on random fractal composites

Do Hoang Ngoc Anh[1], **P Blaudeck**[1], **K H Hoffmann**[1], **J Prehl**[1] **and S Tarafdar**[2]

[1] Institut für Physik, Technische Universität, 09107 Chemnitz, Germany
[2] Condensed Matter Physics Research Centre, Jadavpur University, Kolkata 700 032, India

Received 16 March 2007, in final form 9 August 2007
Published 4 September 2007
Online at stacks.iop.org/JPhysA/40/11453

Abstract

Stochastic fractals, generated from combinations of deterministic fractals, have the advantage of being tractable to some extent, but also being closer to real materials, since they are partially disordered. In the present work, we focus our attention on the remarkable nonlinear mixing behavior exhibited by fractals generated as random combinations of two different Sierpinski carpet generators. When patterns with different anomalous diffusion exponents and the same or different fractal dimensions are combined together, the effective diffusion exponent cannot in general be expressed as a linear weighted average of the diffusion exponents of the constituents. The effective exponent may show a maximum or minimum for certain compositions. An explanation of this interesting phenomenon is offered on the basis of details of the carpet generator, particularly on the number and position of 'connection points', which determine the connectivity of the 'fractal composite'.

PACS numbers: 61.43.Hv, 66.30.−h

1. Introduction

Mixtures or composites of two different materials with varying proportions are generally expected to follow Vegard's law [1]. That is, suppose a property X has different values for components 1 and 2, the effective X for a mixture is usually given by

$$X(\text{eff}) = xX(1) + (1 - x)X(2), \tag{1}$$

where x and $(1 - x)$ are the fractions in which components 1 and 2 are mixed. This implies a linear variation between $X(1)$ and $X(2)$, which is indeed observed in several properties of composites and alloys. However, nonlinear behavior [2] is also encountered in many cases, e.g. in electrical, dielectric and elastic properties of composites. This behavior is difficult to explain from mean field theories, often percolation-type [3] phenomena are responsible. Such effects are well known in ion conductors, when an insulator is dispersed into a poor conductor, a remarkable increase in ion conductivity is observed [4], on the other hand two different

ion-conducting glasses with fairly good conduction properties show very poor conduction when mixed together [5, 6].

In the present work, we report this type of behavior in diffusive properties of a 'fractal composite'. A fractal with a certain structure is characterized by its diffusion exponent d_w defined below. We show that when two fractals with different d_w are mixed to form a composite the effective d_w does not necessarily follow Vegard's law. The composite fractal may have better or worse conducting properties than its constituents. We simulate several such composites and investigate anomalous diffusion on them. We try to explain on the basis of the structural details of the generators, in which case the composite will conduct better and in which case worse. Since many real materials exhibit fractal structure [7, 8], we expect this study to be of practical importance for disordered systems.

The diffusion behavior on fractal structures [9] is different from normal diffusion. It is known that in the case of a Euclidean lattice, i.e. normal diffusion, the mean square distance $\langle r^2 \rangle$ traveled by diffusing particles at time step t is given by

$$\langle r^2 \rangle = Dt, \tag{2}$$

where the constant D is the diffusion coefficient. However, on fractal structures, the mean square displacement is no longer proportional to the time, but

$$\langle r^2 \rangle \propto t^{\gamma}, \tag{3}$$

where $\gamma = \frac{2}{d_w}$ is the anomalous diffusion exponent and d_w is the random walk dimension of the fractal. In the case of normal diffusion, d_w equals 2, so that $\gamma = 1$, hence the scaling relation becomes linear and coincides exactly with (2). When $d_w \neq 2$, diffusion is said to be anomalous.

In fractals, the random walk exponent is usually greater than 2, what implies sub-diffusive behavior, which means that on average the walker moves slower than at normal diffusion. In general, such diffusive behavior is studied though performing random walk simulations.

Anomalous diffusion, particularly *sub-diffusion* has been extensively studied. The earlier literature is reviewed in [9, 10]. Interest in the topic continues and more recent studies show that sub-diffusion may be induced by disorder [11]. The survival probability of sub-diffusive walkers in the presence of traps is simulated by Ruiz-Lorenzo *et al* [12]. Sub-diffusion of colloidal particles near the glass transition is discussed in [13]. The role of sub-diffusion in surface diffusion is discussed by Sancho *et al* [14].

In fact, Klafter and Sokolov [15] suggest that anomalous diffusion is the rule rather than the exception in the natural world. In support, they cite the widespread occurrence of sub-diffusion observed from the flight patterns of birds to the distribution of proteins in biological membranes and even the working of photocopier machines.

Another important property of fractals is the 'fractal dimension' d_f, which expresses the scaling relation between its 'mass' M and 'radius' r:

$$d_f = \frac{\log M}{\log r}. \tag{4}$$

In order to model disordered structures, regular fractals like Sierpinski carpets (SC) are often used [16]. The SC is a particularly simple model, which can be created in a wide variety of patterns with finite or infinite ramification. It is a two-dimensional model but may be generalized to three dimensions as variations of the Menger sponge [16]. Regular SCs are characterized by a particular generator. In the present work, we consider randomized SC that are based on different generators. The diffusion properties of the regular SC generated by single patterns have already been studied [17, 18].

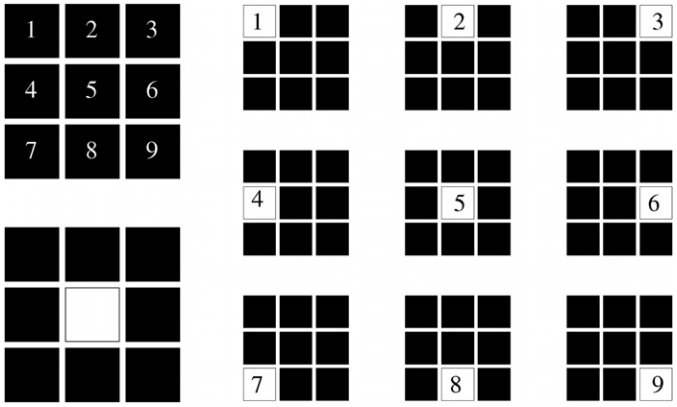

Figure 1. (Left) Order of subsquares and the classic Sierpinski generator; (right) different generators, each with another removed subsquare.

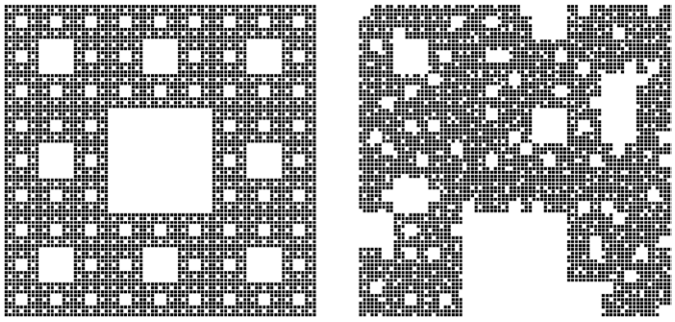

Figure 2. Carpet at the third level: (left) classic regular SC; (right) related random SC.

A generator is a square, divided into $n \times n$ congruent subsquares, where m of them are labeled black and $n^2 - m$ are labeled white. In our model, the black squares are 'allowed' sites and the white are 'blocked'. Figure 1 illustrates examples of a generator. Here, the square is divided into 3×3 makes 9 equal subsquares, and if, for example, the subsquare with number 5 is removed, the result is a single generator. In creating a regular fractal, this generator will be applied repeatedly. The black subsquares remain, whereas the white ones are removed and, in the next iteration stage, each black square is again divided into $n \times n$ equal subsquares and the pattern of the generator is applied on it. This construction procedure repeated *ad infinitum* generates the self-similar regular SC. If we stop the iteration process at the third stage, we will get the SC shown in figure 2 (left). In this example, the 'mass' of the SC is equal to the number of black squares (here 8^3), while its 'radius' equals its linear size (here 3^3). With (4), we determine the fractal dimension of the given SC as

$$d_{\mathrm{f}} = \frac{\log m}{\log n} = \frac{\log 8^3}{\log 3^3} = 1.8928. \tag{5}$$

However, the deterministic model does not capture the randomness of the local fractal structure present in real materials. A more appropriate model is thus based on random fractal structures. In contrast to the regular one constructed above, *random* fractals with the same

'mass' can be generated. For this purpose, it is necessary to change the generator randomly by removing incidentally another subsquare out of the given nine, instead of always the fifth one. As an example, in the first iteration stage the black square is divided into 3×3 subsquares and one of the subsquares (number 8) is removed. In the next level, this procedure is repeated with the eight remaining subsquares, but in each subsquare a different subsquare is removed at random. In other words, a random mixture of the generators in figure 1 (right) is used. At the third iteration level, this procedure results in the random fractal shown in figure 2 (right). This SC is similar to that constructed by Ben-Avraham and Havlin [9]. In 1996, Reis studied random walks on such structures [19]. He analyzed the scaling properties of the mean square displacement after N-step walks and investigated the anomalous diffusion exponents. He found that the exponents obtained are very close to the estimates for the carpets with the same fractal dimension.

Recently [20], we performed a similar investigation. But our construction of the random fractal, and, therefore, our results are quite different from Reis. The main difference is that we have used mixtures of *only two* generators in the iterative creation of each random fractal structure. One important result is that even carpets originated from mixtures of generators with the same d_f and d_w show variations in their observed effective d_w.

In this paper, we continue the simulations in [20], but with rather different patterns of generators. In addition to our former results, some new and interesting behaviors are observed. We show that combinations of a particular pattern with its rotated 'image' are not the same if the rotating angle is different. We have also turned our attention closer to geometrical properties such as traps and shortest paths for crossing over a cell. These new results will be discussed in detail below.

It must be kept in mind, however, that two-dimensional modeling of real three-dimensional systems can at most have limited success. Problems involving connectivity, such as percolation [3], are very different in two and three dimensions. A little reflection makes this clear, e.g. in a random system composed of 'black' and 'white' sites, in 2D it is not possible to have a bi-connected system, where both the black and white sites simultaneously percolate along both the X- and Y-directions. But such a situation can easily be visualized in 3D. So we do not expect the results of the present 2D simulations to be directly comparable to experimental results, but they should nevertheless throw some light on the problem.

2. Connection points and anomalous diffusion

In the previous section, we showed the SC as a particular case belonging to one class of deterministic fractals in the two-dimensional Euclidean space. Much work has been done in this field, focused on modeling porous materials [18, 21] and diffusion on it [10, 17, 22].

Regular random SCs are constructed by applying at least two generators, instead of only one in deterministic cases. Generating a regular random fractal, first we select a generator at random for the first iteration step. The resulting structure is called a 'cell' and all black squares in the cell are referred to 'active sites' of this one. In the next iteration step, for each subsquare of a cell a generator is chosen at random from the given set. Again, these generators are applied to each black subsquares resulting in sub-subsquares labeled according to the selected generator. During this iteration step, the subsquares become cells. This construction procedure could be repeated *ad infinitum*, but in practice it is stopped at a finite iteration depth l.

Cells contain some special sites which we call *connecting points*. A connecting point is a black square that has neighboring sites on different cells. In figure 3, these connections are marked by white arrows. The neighbor is also a connecting point of its cell. Connecting points

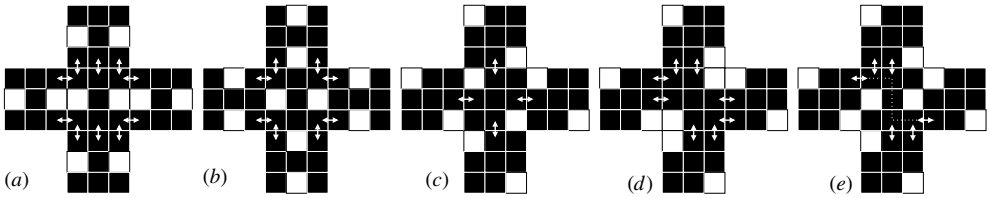

Figure 3. Active connections for several circumstances.

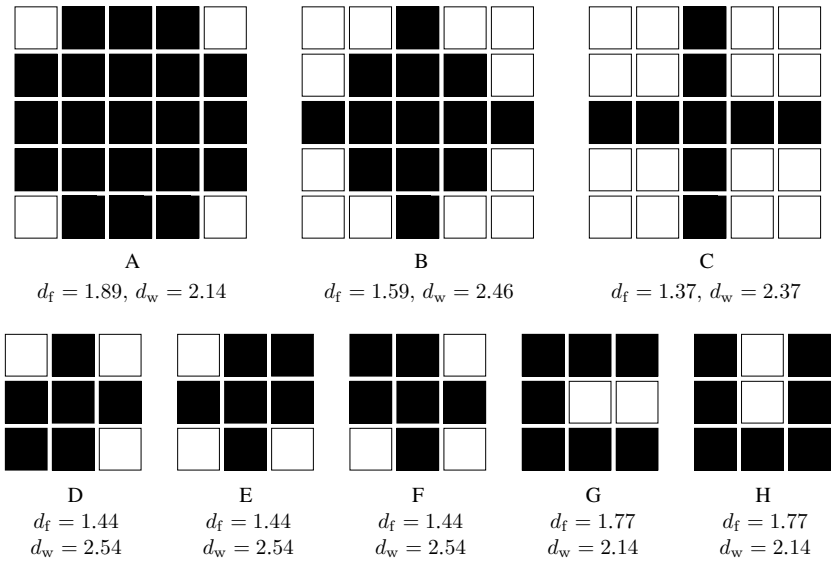

Figure 4. The generators A–H used for constructing carpets.

may be single or double. Single connecting points have only one neighbor in another cell. Double connecting points are connected with two different connecting points of two different cells and can only be found at corners of cells. The more connections a cell has, the higher the probability to contact with other cells. We define C_p as the total number of connections from a cell to its neighbors.

3. Modeling carpets and calculating diffusion exponents

In this work, we use eight generators in total, named A, B, . . . , H, and mix them in pairs to create random fractals. Generators A, B and C are of size 5×5 and the rest are 3×3. Generator E is obtained by rotating D by 90° clockwise, generator G is the result of a 180° rotation of D and generator H is obtained by rotating F counterclockwise by 90°. The generators are shown in figure 4.

From 5×5 generators A, B and C, we constructed 11 combinations for each pair of generators: A_xC_{100-x} and B_xC_{100-x}. With 3×3 generators D, E, F, G and H, we created 11 combinations for each pair that gives D_xE_{100-x}, D_xG_{100-x}, F_xD_{100-x} and F_xH_{100-x} with

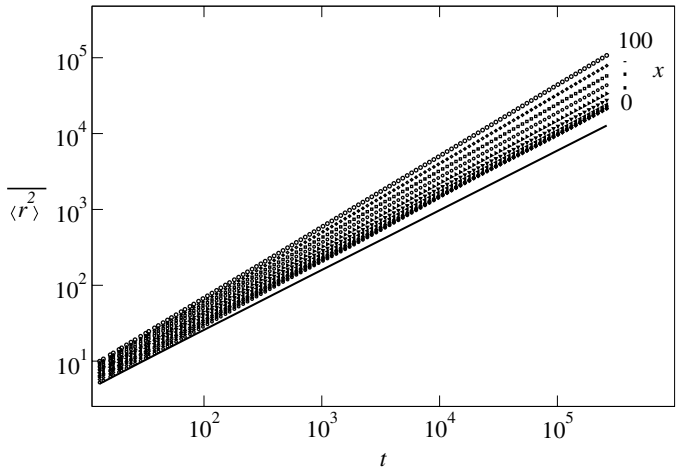

Figure 5. Log–log plot of the mean-squared displacement: (solid line) fractal $D_{40}E_{60}$; (symbols) fractals A_xC_{100-x} for $x = 0, \ldots, 100$.

$x = \{0, 10, 20, \ldots, 100\}$. To obtain a good average for d_w of the random walk simulation, we created $\nu = 100$ different carpets for each combination.

We iterated 5×5 carpets up to level $l = 6$ and 3×3 carpets up to level $l = 8$. Then we combine carpets with identical copies of itself in all space directions in order to get homogeneous structures for large length scales.

The diffusion is investigated by performing random walks on these carpets using the blind ant algorithm. At each time step t_i, the jth walker chooses one random direction out of four (upward, downward, to the left and to the right) with equal probability (25%). If the neighbor square in the selected direction is allowed, the walker will move to that site, otherwise it will stay and wait for an opportunity to move in the next time step. For each time step, we determine the squared distance from its initial site (end-to-end vector) in order to obtain the average value of $\langle r^2(t_i)\rangle$ over N walkers as a function of time

$$\langle r^2(t_i)\rangle = \frac{1}{N}\sum_{j=1}^{N} r_j^2(t_i) - \left(\frac{1}{N}\sum_{j=1}^{N} r_j(t_i)\right)^2, \tag{6}$$

where $t_i = (\sqrt[8]{2})^i$, $i = 56, \ldots, 144$ with $t_{\max} = (\sqrt[8]{2})^{144} = 262\,144$. Using these data, we get $\langle r^2\rangle_{\max} < 10\,000$ and thus r with a typical order of $r \approx 100$. This value of r guarantees that walkers still walk within the first iterator after $t_{\max}$ time steps, and thus $\langle r^2\rangle$ has not been seriously affected by boundaries. To avoid the fluctuations due to the local geometry of a particular sample, we take the average of $\langle r^2\rangle_k$ over ν realizations of random fractals:

$$\overline{\langle r^2\rangle} = \frac{1}{\nu}\sum_{k=1}^{\nu}\langle r^2\rangle_k. \tag{7}$$

For each realization, we use $N = 20\,000$ walkers for a good approximation. The solid line in figure 5 shows a typical $\overline{\langle r^2\rangle}$ versus time plot, it is a rather straight line. Thus, the randomness of the fractal does not alter the anomalous diffusion behavior with a power-law time behavior.

Table 1. Simulation results for the mixtures A_xC_{100-x} and F_xD_{100-x}.

	d_w			d_w	
x	A_xC_{100-x}	F_xD_{100-x}	x	A_xC_{100-x}	F_xD_{100-x}
0	2.370 180	2.541 347	22	2.446 839	2.600 957
10	2.413 639	2.578 367	24	2.448 649	2.601 136
20	2.443 633	2.597 414	26	2.451 049	2.601 783
30	2.456 525	2.601 529	28	2.454 077	2.601 740
40	2.450 712	2.592 068	30	2.456 525	2.601 529
50	2.430 566	2.565 014	32	2.454 541	2.600 591
60	2.391 684	2.524 204	34	2.454 489	2.599 686
70	2.334 419	2.465 063	36	2.452 853	2.595 916
80	2.271 119	2.383 253	38	2.452 963	2.594 276
90	2.201 776	2.277 535			
100	2.135 509	2.139 521			

From the slope of these straight lines in log–log plots of $\overline{\langle r^2 \rangle}$ over time, we can calculate the random walk dimension d_w:

$$\overline{\langle r^2 \rangle} \propto t^{\gamma} \quad \Rightarrow \quad \gamma \propto \frac{\log \overline{\langle r^2 \rangle}}{\log t} \quad \Rightarrow \quad d_w = \frac{2}{\gamma}. \tag{8}$$

4. Results and discussion

4.1. Diffusion decreases when mixing generators

Table 1 shows the resulting d_w as a function of the percentage x of generator A in combinations A_xC_{100-x} and percentage x of generator F in combinations F_xD_{100-x}. The value of d_w reaches a peak which can clearly be seen in the top of figure 6. To locate the maximum to a higher degree of precision, we additionally analyzed the fractions x as shown in the right-half of table 1.

First, we consider the combinations of A_xC_{100-x}. Starting at $x = 0$, we can observe an increase of d_w from 2.3702 to 2.4565 at $x = 30$, followed by a decrease to 2.1356. This behavior can be explained as follows.

When $x = 0$, all cells of the carpet are labeled according to generator C, which is a regular SC created by generator C with $C_p = 4$ for each cell. While x is increasing, some cells, which were occupied by generator C, are replaced by generator A. If a cell A is put among 4 cells C, its C_p still equals 4, but the number of active sites increases from 9 to 21. In this range of x, the number of cells A surrounded by cells C is much larger than the number of cells C surrounded by cells A. Consequently, the walkers have to walk more often inside a cell before they can escape through one connecting point. Therefore, the velocity of the diffusion drops to the slowest value at $x \approx 30$. But, as x continues to rise to 100, the C_p of one cell also increases from 4 to 12. Thus, a walker has more opportunities to escape from one cell to another. So, the diffusion velocity increases and d_w decreases.

We obtained a similar curve for the combinations F_xD_{100-x} in the right part of figure 6. When $x = 0$, all cells of the carpet are marked by generator D. Each cell has $C_p = 4$ and 6 allowed squares. As x increases, some cells F replaces cells D and they are surrounded by a number of cells D. If a cell F is put among four cells D, we can observe that $C_p = 5$ and we

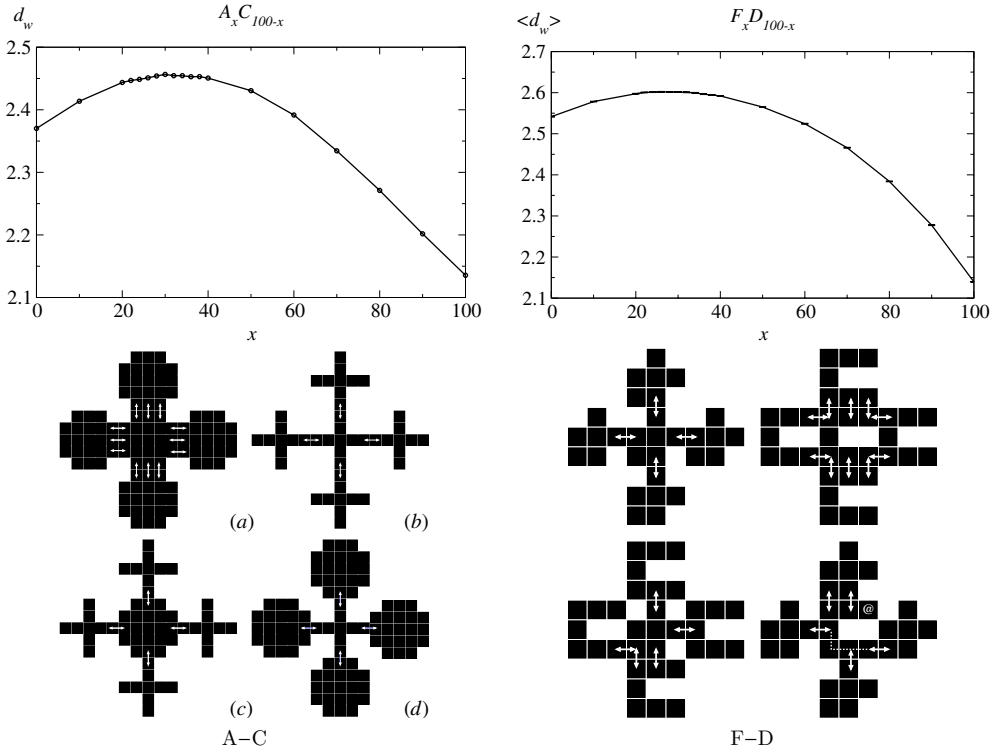

Figure 6. Results for mixtures A–C and F–D: (top) $d_w(x)$; (middle) original carpets; (bottom) mixtures with changed connecting points (marked by arrows).

have seven black sites in the cell. Here, C_p increases, but due to the shape of generator F, the shortest path through the cell also increases from 3 to 4, if walker travels along the horizontal or vertical direction. The randomness also creates a 'dead-end' site, which is marked by a dot in figure 6(*h*). Longer shortest paths, 'dead-end' sites and a larger number of active sites are reasons for the increase of d_w from 2.5413 to 2.6018, while x reaches 26. As x continues to go up, more and more cell F appears. In other words, we have a higher probability to find a cell D amid four cells F. Here, C_p still equals 5, but the 'dead-end' site disappears. The shortest path to travel along the horizontal direction is still 4, but the shortest path traveling along the vertical direction falls to 3, hence d_w decreases. When x rises to 100, we can find only cells F, the shortest path along each direction drops to 3 and C_p raises to 10. Therefore, d_w decreases, i.e. the diffusion velocity increases.

4.2. Strange behaviors—diffusion enhanced

Table 2 and figure 7 show the resulting average d_w as a function of the percentage x of generator F in combinations F_xH_{100-x} and the corresponding function of the percentage x of the generators D in combinations D_xG_{100-x}. These two cases are quite different in comparison to the simulations in the previous section. We can see that both curves are symmetric according to $x \approx 50$, where the curves reach their extremum. But in contrast to all other cases the

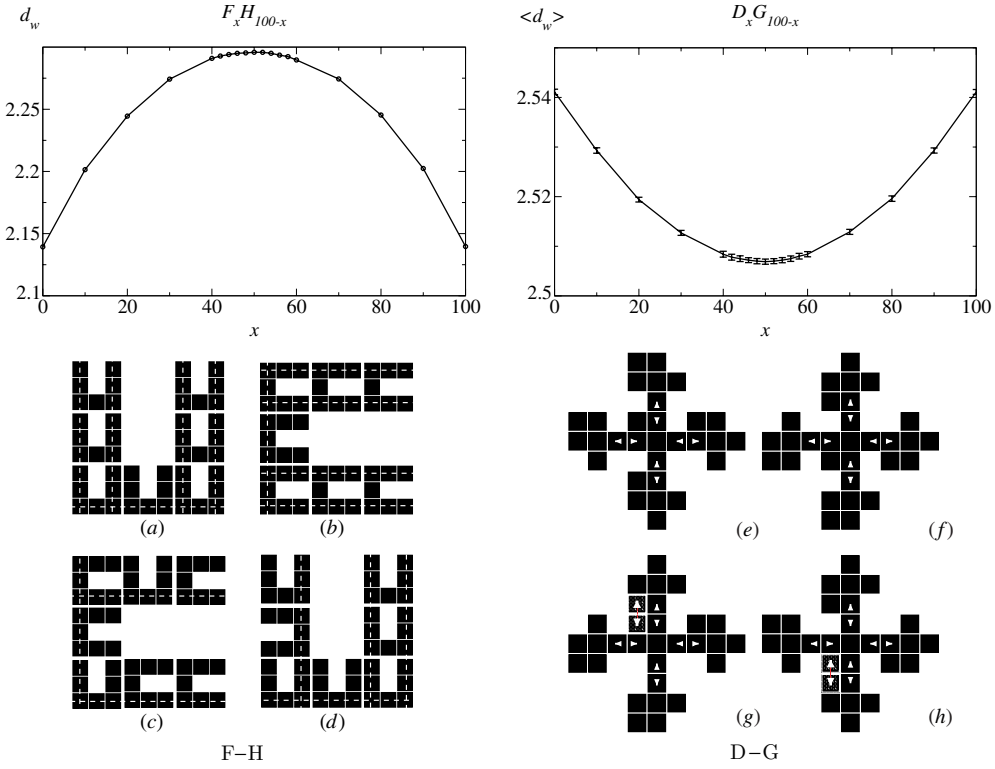

Figure 7. Results for mixtures F–H and D–G: (top) $d_w(x)$; (middle) original carpets; (bottom) mixtures with changed connecting points (marked by arrows) and shortest paths (dashed lines).

Table 2. Simulation results for the mixtures F_xH_{100-x} and D_xG_{100-x}.

	d_w			d_w	
x	F_xH_{100-x}	D_xG_{100-x}	x	F_xH_{100-x}	D_xG_{100-x}
0	2.139 345	2.541 081	40	2.290 930	2.508 936
10	2.201 471	2.528 773	42	2.292 812	2.507 315
20	2.244 527	2.518 822	44	2.294 020	2.507 591
30	2.274 242	2.512 547	46	2.294 986	2.507 018
40	2.290 930	2.508 936	48	2.295 349	2.507 021
50	2.295 841	2.506 715	50	**2.295 841**	**2.506 715**
60	2.289 660	2.507 847	52	2.295 802	2.507 078
70	2.274 382	2.513 084	54	2.295 030	2.507 173
80	2.245 373	2.520 011	56	2.293 531	2.507 129
90	2.202 372	2.529 458	58	2.292 342	2.507 570
100	2.139 616	2.540 945	60	2.289 660	2.507 847

combinations of D_xG_{100-x} exhibit a minimum, which implies that diffusion of this mixture is faster than it is on the pure SCs.

The symmetry of the two curves results from the choice of the pairs of generators. As we mentioned before, generator H is generator F rotated by 90°. The same holds for generator

G, which is the 90° rotated generator D. In other words, when we rotate the hole SC based on generator F (or D), we will get the SC based on generator H (or G). Therefore, $F_u H_{100-u}$ and $F_{100-u} H_u$ with $0 \leqslant u \leqslant 100$ are equivalent to each other.

Analyzing d_w of the mixture of generators F and H, we found that C_p of each cell is statistically 10 and the shortest path to cross a cell is always 3. In order to explain the changes of d_w for different mixing ratios, we have to investigate the number of shortest paths. This must be done not only in the smallest cell (last iteration level), but also for the cells according to a higher level of iteration (illustrated in figures 7(*a*) and (*b*)). At $x = 0$, generator H occupies all cells of the fractal. Figure 7(*a*) illustrates a part of such a carpet, which coincides with one cell H. Dashed lines exhibit all possible shortest paths that walkers could use to travel across the cell. We can observe four vertical lines and one horizontal one, which leads to five lines in total. As x increases, some cells of H will be replaced by cells F. This creates defects in the self-similarity structure and breaks one or two shortest paths. For higher values of x, more cells H are replaced, so more defects appear and less dashed lines can be observed. Hence the number of total shortest paths decreases from five to four (figure 7(*d*)) to three (figure 7(*c*)). For this reason, it takes more time for the walkers to travel through a cell, thus the velocity of the diffusion also decreases. When $x = 50$, the distribution of cells F and H are evenly distributed and cells like in figure 7(*a*) can be observed rarely. In most of the cases, we can find cells with only three dashed lines and therefore the diffusion reaches the lowest value. If x continues to go up, F cells occur more and more and the number of dashed lines can increase. So d_w decreases, i.e. the diffusion gets faster. When $x = 100$, only generator F occupies all cells in the carpet and again we find five dashed lines (figure 7(*b*)).

A completely different behavior is shown in the third and sixth columns of table 2 and in the upper-right of figure 7. Here, the mixtures of generators D and G are presented. d_w exhibits a minimum at $x = 50$. The very surprising result is that diffusion is *enhanced* rather than slowed down by increasing disorder. Again, the above reasoning helps us to understand this behavior. In the cases of the pure SCs, each cell has $C_p = 4$. But this number will change if some cells G are replaced by cells D and one of the new cells is put 'above' one cell G. In figures 7(*g*) and (*h*), we can observe five instead of four connections. At $x = 50$, cells D and G are distributed uniformly. The probability to find a cell D or a cell G are equal and further on the probability to find a cell D placed above cell G reaches its maximum, therefore C_p is maximal in the whole carpet. Consequently, the walkers have more possibilities to escape out of a cell and so they travel faster. Therefore, d_w decreases and thus the diffusion will be enhanced.

In three of the four mentioned cases (A–C, F–D, F–H), C_p of each combination is always equal to or less than the C_p of the original SCs, whereas in the case of D–G the C_p of the combinations is always larger than that of the pure ones. So, in general, we find that decreasing C_p induces an increase of d_w with a maximum at a certain mixing ratio, and increasing C_p leads to a decrease of d_w and a minimum will appear.

It may be noted that if the basic generator is anisotropic, such nonlinear effects are more likely to show up, e.g. in the combinations of F–H in figure 7, the difference between d_w for the pure systems (2.14), from the 50% mixture is 0.15, which is quite significant. The pair D–G on the other hand, is relatively more isotropic, here the difference (in this case negative) is of magnitude 0.04, much smaller compared to 2.54, for the pure systems.

4.3. Other cases

In contrast to the previous cases, we show two more simulations by mixing the generators B and C as well as D and E, respectively, which exhibit a quite different behavior. Table 3

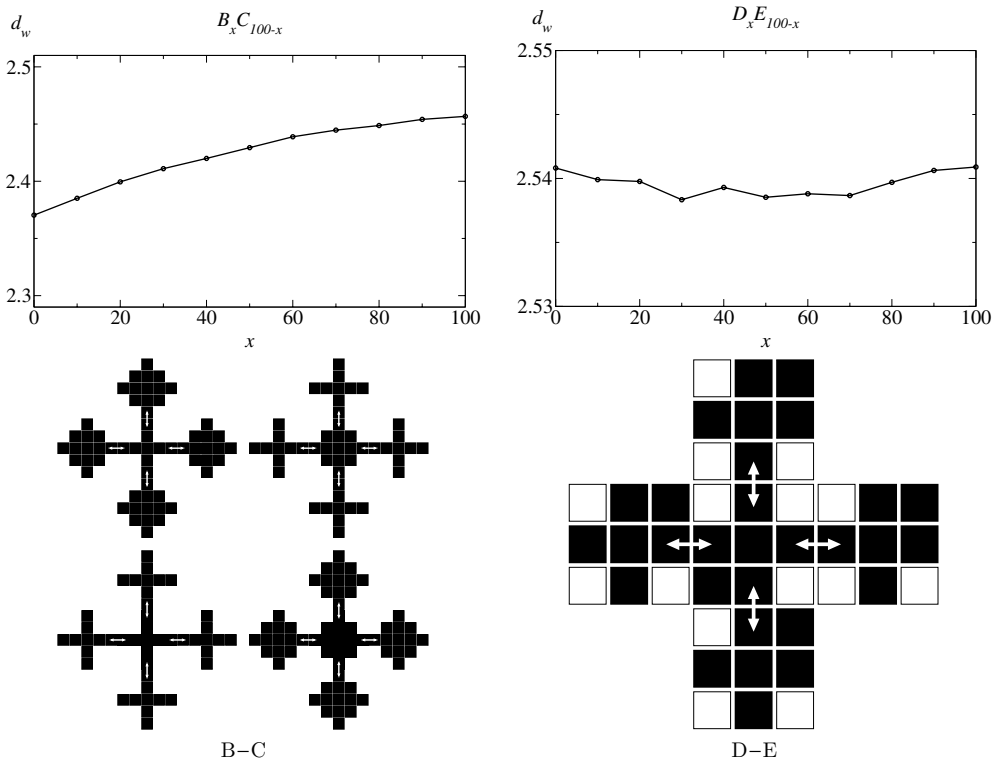

Figure 8. Results for mixtures B–C and D–E: (top) $d_w(x)$; (bottom) mixtures with connecting points (marked by arrows).

Table 3. Simulation results for the mixtures B_xC_{100-x} and D_xE_{100-x}.

	d_w	
x	B_xC_{100-x}	D_xE_{100-x}
0	2.370 363	2.540 817
10	2.385 102	2.539 910
20	2.399 458	2.539 766
30	2.410 993	2.538 337
40	2.419 952	2.539 296
50	2.429 398	2.538 529
60	2.438 875	2.538 803
70	2.444 701	2.538 664
80	2.448 729	2.539 696
90	2.454 084	2.540 625
100	2.456 737	2.540 893

and figure 8 show the resulting average d_w as a function of the percentage x of generator B in combinations B_xC_{100-x} and D_xE_{100-x}. These functions d_w are different from any previous cases. In figure 8, we can see the curve for the combinations B_xC_{x-100} starting for $x = 0$ with $d_w = 2.3703$ and increasing to 2.4567 for $x = 100$ without observing any extremum. This

behavior can be understood by the following explanation. While mixing B and C, in all cases only four single connecting points appear and the length of the shortest paths is always 5. So the increase of the number of active sites from 9 to 13 is the only reason for the shift of d_w between the two original d_w.

In the last case, where we mix generators D and E, no significant curvature for d_w occurs. In fact, a horizontal line within the statistical fluctuation appears. There is neither a maximal nor a minimal value. That is, due to the chosen generators, both patterns have the same d_w and d_f. The number of connection points ($C_p = 4$), the length of the shortest path and the number of active sites are equal for both generators. That is, also the case if we mix these generators, all values remain constant. So nothing changes inside the random fractal and we get the horizontal line for d_w.

5. Conclusions

We studied random SCs by mixing pairs of different generators. The investigation of several mixtures with varying composition shows that such structures display a power-law relation similar to completely deterministic fractals, and random walks are characterized by an exponent d_w.

We have shown that the effective diffusion properties of a mixture of two different deterministic fractals is not necessarily a linear combination of the properties of the constituents. The diffusion exponent may be enhanced, implying a worse diffusivity, or reduced, implying better diffusivity of the composite, compared to both the constituents. An explanation of which effect prevails, can be offered, by scrutinizing the 'connecting points' which provide access from one fractal cell to the next. This fact emphasizes the role of the detailed geometry of the components, rather than an average property such as the fractal dimension d_f. Combinations more likely to provide a spanning percolation path through the whole system, provide better diffusivity.

References

[1] Denton A R and Ashcroft N W 1991 Vegards law *Phys. Rev.* A **43** 3161–4

[2] Liou B T, Yen S H and Kuo Y K 2005 Vegards law deviation in band gap and bowing parameter of $Al_xIn_{1-x}N$ *Appl. Phys.* A **81** 651–5

[3] Stauffer D and Aharony A 1994 *Introduction to Percolation Theory* (London: Taylor and Francis)

[4] Liang C C 1973 Conduction characteristics of the lithium iodide–aluminum oxide solid electrolytes *J. Electrochem. Soc.* **120** 1289–92

[5] Isard J O 1969 The mixed alkali effect in glass *J. Non-Cryst. Solids* **1** 235–61

[6] Ingram M D 1987 Ionic conductivity in glass *Phys. Chem. Glasses* **28** 215–34

[7] Roy S, Dasgupta R and Tarafdar S 1996 A fractal model for superionic aerogels *Solid State Ion.* **86–88** 363–7

[8] Dutta T and Tarafdar S 2003 Fractal pore structure of sedimentary rocks: simulation by ballistic deposition *J. Geophys. Res.* **108** 2062

[9] Ben-Avraham D and Havlin S 2000 *Diffusion and Reactions in Fractals and Disordered Systems* (Cambridge: Cambridge University Press)

[10] Bouchaud J P and Georges A 1990 Anomalous diffusion in disordered media: statistical mechanisms, models and physical applications *Phys. Rep.* **195** 127–293

[11] Bertin E M and Bouchaud J-P 2003 Subdiffusion and localization in the one-dimensional trap model *Phys. Rev.* E **67** 026128

[12] Ruiz-Lorenzo J J, Yuste S B and Lindenberg K 2007 Simulations for trapping reactions with subdiffusive traps and subdiffusive particles *J. Phys. C: Solid State Phys.* **19** 065120

[13] Weeks E R and Weitz D A 2002 Subdiffusion and the cage effect studied near the colloidal glass transition *Chem. Phys.* **284** 361–7

[14] Sancho J M, Lacasta A M, Lindenberg K, Sokolov I M and Romero A H 2004 Diffusion on a solid surface: anomalous is normal *Phys. Rev. Lett.* **92** 250601
[15] Klafter J and Sokolov I M 2005 Anomalous diffusion spreads its wings *Phys. World* **18** 29–32
[16] Mandelbrot B B 1977 *Fractals—Form, Chance and Dimension* (San Francisco: Freeman)
[17] Schulzky C, Franz A and Hoffmann K H 2000 Resistance scaling and random walk dimensions for finitely ramified Sierpinski carpets *SIGSAM Bull.* **34** 1–8
[18] Franz A, Schulzky C, Tarafdar S and Hoffmann K H 2001 The pore structure of Sierpinski carpets *J. Phys. A: Math. Gen.* **34** 8751–65
[19] Aarão Reis F D A 1996 Diffusion on regular random fractals *J. Phys. A: Math. Gen.* **29** 7803–10
[20] Anh D H N, Hoffmann K H, Seeger S and Tarafdar S 2005 Diffusion in disordered fractals *Europhys. Lett.* **70** 109–15
[21] Tarafdar S, Franz A, Schulzky S and Hoffmann K H 2001 Modelling porous structures by repeated Sierpinski carpets *Physica* A **292** 1–8
[22] Seeger S, Franz A, Schulzky C and Hoffmann K H 2001 Random walks on finitely ramified Sierpinski carpets *Comput. Phys. Commun.* **134** 307–16